The satiety hormone cholecystokinin gates reproduction in fish by controlling gonadotropin secretion

Lian Hollander Cohen[1], Omer Cohen[1], Miriam Shulman[1], Tomer Aiznkot[1], Pierre Fontanaud[2,3], Omer Revah[5], Patrice Mollard[2,3], *Matan Golan[4] & *Berta Levavi Sivan[1].

*Matan Golan: matang@volcani.agri.gov.il
*Berta Levavi Sivan: Berta.sivan@mail.huji.ac.il

(1) Department of Animal Sciences, The Robert H. Smith Faculty of Agriculture, Food, and Environment, Hebrew University of Jerusalem, Rehovot 76100, Israel.
(2) Institute of Functional Genomics, University of Montpellier, CNRS, INSERM, France.
(3) BioCampus Montpellier, University of Montpellier, CNRS, INSERM, F-34094 Montpellier, France.
(4) Department of Poultry and Aquaculture, Institute of Animal Sciences, Agricultural Research Organization, Volcani Center, P.O.B 15159, Rishon Letziyon 7505101, Israel.
(5) The Koret School of Veterinary Medicine, The Hebrew University of Jerusalem, Jerusalem, Israel

Abstract
Life histories of oviparous species dictate high metabolic investment in the process of gonadal development leading to ovulation. In vertebrates, these two distinct processes are controlled by the gonadotropins follicle-stimulating hormone (FSH) and luteinizing hormone (LH), respectively. While it was suggested that a common secretagogue, gonadotropin-releasing hormone (GnRH), oversees both functions, the generation of loss-of-function fish challenged this view. Here we reveal that the satiety hormone cholecystokinin (CCK) is the primary regulator of this axis in zebrafish. We found that FSH cells express a CCK receptor, and our findings demonstrate that mutating this receptor results in a severe hindrance to ovarian development. Additionally, it causes a complete shutdown of both gonadotropins secretion. Using *in-vivo* and *ex-vivo* calcium imaging of gonadotrophs, we show that GnRH predominantly activates LH cells, whereas FSH cells respond to CCK stimulation, designating CCK as the bona fide FSH secretagogue. These findings indicate that the control of gametogenesis in fish was placed under different neural circuits, that are gated by CCK.

Introduction
In vertebrates, the processes of folliculogenesis, ovulation and spermatogenesis are controlled by two gonadotropin hormones (GtHs), follicle-stimulating hormone (FSH) and luteinizing hormone (LH). In fish, different loss-of-function (LOF) studies revealed the stereotyped function of each gonadotropin: FSH signaling controls folliculogenesis, whereas the role of LH is restricted to the induction of ovulation (*2-4*). According to the existing dogma, the secretion of both GtHs by gonadotrophs of the anterior pituitary gland is controlled by the hypothalamic neuropeptide gonadotropin-releasing hormone (GnRH), which is produced by a small population of neurons in the preoptic area (*5*). Studies conducted in mammals have shown that the differential control over

gonadotropin secretion is attained via changes in frequencies and amplitude of GnRH pulses (*6-8*), as well as by a variety of other endocrine and paracrine factors that dictate whether the cells will secrete LH or FSH. In fish, the TGF-β family members activin, inhibin, and follistatin, as well as PACAP signalling have been shown to exert a differential effect on FSH and LH synthesis (*9-12*). However, the hypothalamic mechanisms governing the differential release of FSH or LH in non-mammalian vertebrates remain largely unknown.
As in mammals, GnRH is considered the master regulator of gonadotropin secretion in fish. However, in recent years, its status as the sole neuropeptide regulating GtH secretion has been called into question, as other hypothalamic neuropeptides were shown to bypass GnRH and directly regulate gonadotropin secretion(*13-21*). Due to genome duplication events, fish brains express up to three forms of GnRH, of which one form (usually GnRH1) innervates the pituitary gland (*22, 23*). In some species, such as the zebrafish, that express only two forms of GnRH (GnRH2 and GnRH3), the gene encoding GnRH1 has been lost, and GnRH3 has become the dominant hypophysiotropic form (*23*). For a yet unknown reason, in the zebrafish, even a complete absence of GnRH does not impair ovulation, as adult zebrafish with loss of function (LOF) of GnRH signaling are fertile (*24-26*), suggesting that GnRH activity is either replaced by a compensation mechanism or it is dispensable for the control of gonadotropin release overall. In other species, such as medaka, the effects of GnRH are limited to the control of final oocyte maturation and ovulation via LH secretion (*2*). Since in both species, the loss of GnRH does not affect gonadal development, the hypothalamic factor controlling FSH secretion in fish remains unknown (*2, 25, 27*)

Here, we addressed the question of the hypothalamic control of LH and FSH secretion in zebrafish. By mutating a previously identified CCK receptor highly expressed in FSH cells (*1*), we prove that CCK controls zebrafish reproduction by gating gonadotropin secretion. Using *in vivo* and *ex vivo* calcium imaging in zebrafish gonadotrophs to identify LH- and FSH-specific secretagogues, we show that the two types of gonadotrophs vary significantly in their activity patterns and that GnRH controls LH cells whereas FSH cells are preferentially activated by the satiety hormone cholecystokinin (CCK), which is also produced in the fish hypothalamus (*28, 29*) and its receptor is highly expressed in FSH cells (*1*). The results identify CCK as a novel crucial regulator of the reproductive axis and establish a direct neuroendocrine link between nutritional status and reproduction in fish.

Results

1.1. CCK and its receptors are vital regulators of the HPG axis

While in mammals, both LH and FSH are secreted by the same cell population, , these gonadotropins are produced by discrete cell types in fish (*1, 30*). We took advantage of this unique feature to search for the mechanism that regulates the differential secretion of LH and FSH in fish. We have previously reported (*1*) that FSH cells differ from LH cells by the expression of an FSH-specific type of cholecystokinin (CCK) receptor. While three types of CCK receptors (CCKRs) are reported in the genome of fish, only one type is expressed in the pituitary gland (*1*). In tilapia, the expression of this receptor is ~100 fold higher in FSH than in LH cells (Fig. 1A). Nevertheless, LH cells also express the CCK receptor albeit at a lower level (Fig. 1A). We therefore first validated its expression

on gonadotroph cells in zebrafish using *in situ* hybridization and found that the receptor is predominantly expressed in FSH cells (Fig. 1B). To identify the source of CCK inputs we used immunohistochemistry to label CCK-expressing cells. We found hypophysiotropic CCK-secreting neuronal projections innervating the pituitary near FSH cells and adjacent to GnRH axons (Fig. 1C), indicating hypothalamic input of CCK into the pituitary gland.

To functionally validate the importance of CCK signalling, we used CRISPR-cas9 to generate loss-of-function (LOF) mutations in the pituitary-specific CCK receptor gene. Three different mutations were induced by guide RNAs designed to target the 4th transmembrane domain of the protein, thus affecting the binding site of the receptor to its ligand (Fig. S1). Three mutations were identified to generate a LOF: insertion of 12 nucleotides (CCKR^{+12}), insertion of seven nucleotides (CCKR^{+7}) and deletion of one nucleotide (CCKR^{-1}). Analysis of the phenotype of F2 adult fish (5-6 months of age) revealed that while non-edited (wt/wt, n=15) and heterozygous fish (wt/CCKR$^{+12/+7/-1}$, n=20) displayed typical sex ratios and functional adult gonads, all homozygous fish (CCKR$^{+12/+7/-1}$/ CCKR$^{+12/+7/-1}$, n=12) were males with significantly small gonads (Fig. 1d-e; mean gonad area KO=3.8±0.48 mm^2, Heterozygous = 23.52± 10.6, WT= 78±7.4 mm^2). The testes of mutant males displayed an immature phenotype as they were populated mostly by early stages of testicular germ cells (mostly spermatogonia and spermatocytes) and contained low volumes of mature spermatozoa compared to their WT and heterozygous siblings (Fig. 1F). Heterozygous fish were also affected and displayed significantly lower amount of spermatozoa compared to the WT fish. Interestingly, the CCK-R LOF fish do not phenocopy zebrafish with a loss of FSH (*31, 32*). Instead, the phenotype of the CCK-R LOF closely resembles the condition reported for zebrafish that have LOF mutations in both gonadotropin genes (*31, 32*). Indeed, our mutants show decreased expression levels of both *lhβ* and *fshβ* genes (Fig. 1G), suggesting that loss of CCK signaling affects both LH and FSH. We next sought to identify the exact effect of the two major HPG regulators GnRH and CCK, on the activity of LH and FSH cells using calcium imaging.

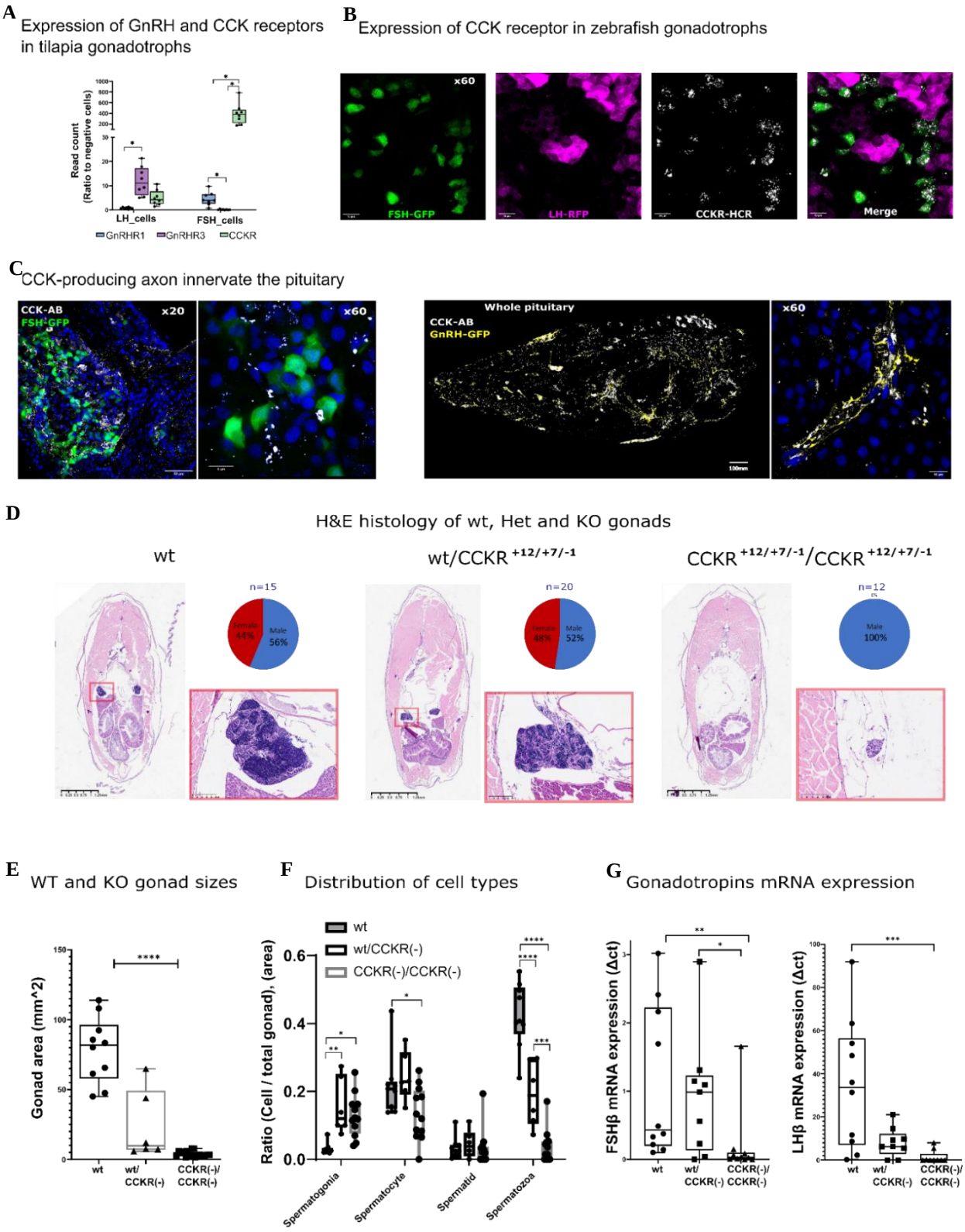

Fig. 1. Effect of CCK-R loss-of-function mutation on gonadal development. (A) Expression of CCKR and two identified GnRH receptors in LH and FSH cells. Expression data were taken from a transcriptome of sorted pituitary cells of transgenic Nile tilapia (*Oreochromis niloticus*), expressing RFP in LH cells and GFP in FSH cells, previously obtained by Hollander-Cohen *et al (1)*. Each dot represents a FACS fraction from a bulk of 20 pituitaries (n=8, 4 groups of males and 4 groups of females). The expression of each gene in each cell type is normalised to its expression in non-gonadotroph pituitary cells. While GnRHR3 is the dominant receptor in LH cells, CCKR has a significantly higher expression in FSH cells (two-way ANOVA, * $p<0.05$,). **(B)** RNA expression of CCKR (white) identified by hybridization chain reaction (HCR) in transgenic zebrafish pituitaries expressing RFP in LH cells (magenta) and GFP in FSH cells (green)

shows specific expression predominanly on FSH cells. **(C)** Immunohistochemical staining of CCK (white) in transgenic zebrafish expressing GFP in FSH cells (left panel) or GFP in GnRH neurons (right panel). The CCK neuronal axons that innervate the pituitary gland are located adjacent to GnRH axons and in very close proximity to FSH cells. **(D)** H&E staining of body cross-sections (dorsoventral axis) of adult WT , heterozygous (wt/ CCKR-$^{+12/+7/-1}$), and KO zebrafish (CCKR-$^{+12/+7/-1}$/ CCKR-$^{+12/+7/-1}$). An inset of the red square in each image on the right displays a magnified view of the gonad. All KO zebrafish exhibit small undeveloped male gonads. On the top right of each panel is the gender distribution for each genotype, while a similar distribution of males and females was identified in the WT and heterozygous; the KO zebrafish were only males. **(E)** Gonad areas of mutant zebrafish. All KO zebrafish exhibit a small gonad compared to the WT and the heterozygous ($n_{((+/+),(+/-),(-/-))}$=10/6/17,one way ANOVA, , ****p<0.0001). **(F)** The distribution of cell types in the gonads of WT, heterozygous and KO zebrafish. CCKR LOF affects the gonad cell distribution and significantly reduces the maturation of the cells to spermatozoa. ($n_{((+/+),(+/-),(-/-))}$=10/6/17, two-way ANOVA, * p<0.05, ** p<0.001, *** p<0.0001 ,****p<0.00001). **(G)** Gonadotroph mRNA expression in the pituitaries of the three genotypes revealed a significant decrease in both LH and FSH beta subunit expression in the KO fish($n_{((+/+),(+/-),(-/-))}$=9/8/10, one-way ANOVA, * p<0.05, ** p<0.01, *** p<0.001) .

1.2. LH and FSH cells exhibit distinct calcium activity in vivo

The unique segregation of LH and FSH cells in fish provides an opportunity to identify genes and pathways that specifically regulate each gonadotroph. To that end, we generated transgenic zebrafish in which both LH- and FSH-producing cells express the red genetically-encoded calcium indicator RCaMP2 (*33*), whereas FSH cells also express GFP (*Tg(FSH:RCaMP2, LH:RCaMP2, FSH:GFP)*; Fig. 2A). These fish allow simultaneous monitoring of calcium activity in LH and FSH cells as a readout for cell activation, while distinguishing between the two cell types.

To follow the activity of LH and FSH gonadotrophs in live zebrafish, we developed a novel preparation for imaging the pituitary gland at single-cell resolution while maintaining the *in vivo* context. In this preparation, the pituitary gland was exposed from its ventral side. The immobilized zebrafish were placed under a two-photon microscope with a constant flow of water over the gills (Fig. 2B), ensuring sufficient oxygen supply to the gills and blood flow to the gland (Movie. S1).

Imaging of the gonadotrophs *in vivo* revealed distinct types of calcium activity in the two cell types (Fig. 2C-E, Fig. S2A). In the basal state LH cells were mostly silent, whereas FSH cells exhibited short (mean of 10.08 sec half width) calcium bursts (mean of 0.6 ΔF/F; Fig 2C (fish1) and d; Movie. S2A). Theses calcium events were sparse, i.e. between 1 and 7 transients in each cell in 10 min, and disorganized, as max cross-correlation coefficient values ranged from 0.3 to 0.9 (Fig. 2E fish1). In 7/10 zebrafish, we observed an event in which LH cells exhibited a single long (mean of 75.55 sec half width) and strong (mean of 1.5 ΔF/F) calcium rise (Fig. 2C (fish2) and d). This event was synchronized between LH cells (mean max cross-correlation coefficient values of 0.89 ± 0.003) and, in 3/7 zebrafish, it was followed by a less synchronized (mean max cross-correlation coefficient values, 0.66 ± 0.011,) calcium rise in FSH cells (Fig. 2C and E (fish2), Movie. S2B). On average, the max cross-correlation coefficient values of all active LH cells were significantly higher compared to FSH cells (Fig. 2F, Fig. S2B), which reflects the stronger coupling between LH cells (*30*). We did not observe significant sexual dimorphism in correlation value distribution in either LH or FSH cells (5 males and 5 females; Fig. S2B). Since most FSH calcium transients were not associated with a rise in calcium in LH cells, we speculated that a cell type-specific regulatory mechanism drives the activity of the two cell types and GnRH and CCK are the primary candidates.

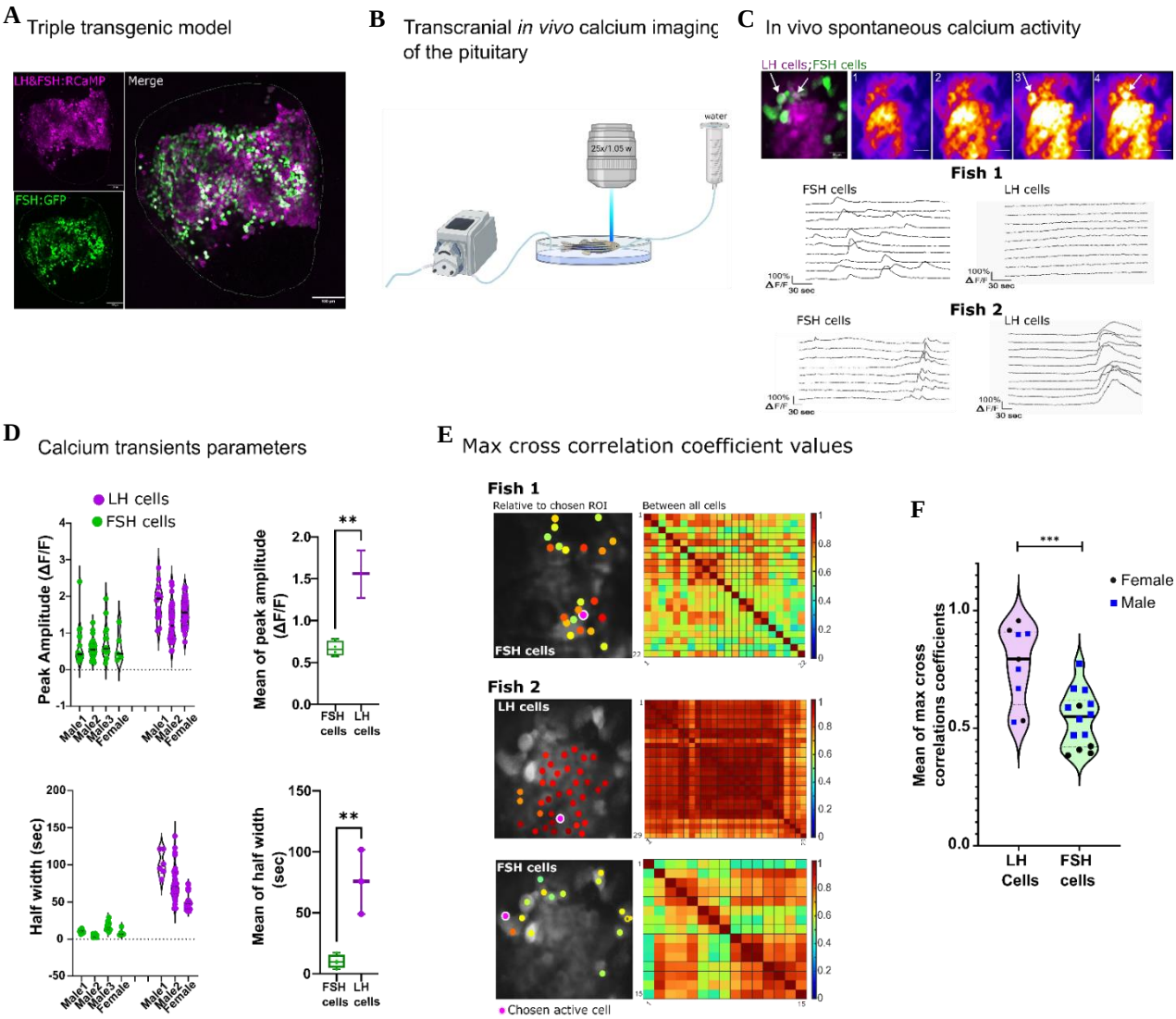

Fig. 2. LH and FSH cells exhibit distinct spontaneous activity patterns *in vivo*. (A) Triple transgenic zebrafish were generated by crossing transgenic zebrafish expressing GFP in FSH cells to zebrafish lines expressing R-CaMP2 in LH and FSH cells. A confocal image of the pituitary shows RCaMP2 expression in both cell types and GFP expression in FSH cells. **(B)** A diagram describing the setup of the *in vivo* experiments. The dissected zebrafish were placed in a chamber with a constant flow of water to the gills and imaged in an upright two-photon microscopy. **(C)** A representative image of *in vivo* calcium activity (see movie. S2). On the top left is a merged image depicting FSH cells in green and LH cells in magenta. The other top panels show sequential calcium imaging, which reveals calcium rise in all LH cells followed by calcium rise in FSH cells (marked by white arrows). The bottom panels show the calcium of LH and FSH cells in two different imaged pituitaries, one where only FSH cells were active (Fish 1) and another where both cell types were active (Fish 2, traces ΔF/F, see supplementary fig. 1a for heatmap of the calcium traces). **(D)** The properties of spontaneous calcium transients (ΔF/F) in LH cells and FSH cells in three males and one female. Means of peak amplitude and duration differed between LH and FSH cells (unpaired *t*-test, ** $p<0.001$). Analysis was performed using pCLAMP 11. **(E)** Left: Cross correlation analysis between active ROI to the rest of the cell. The color-coded data points are superimposed on the imaged cells and represent the maximum cross-correlation coefficient between a calcium trace of a region of interest (ROI) and that of the rest of the cells in the same population. Right: is a matrix of maximum cross-correlation coefficient values between all the cells. All LH cells exhibited highly correlated calcium activity. In comparison, the activity of FSH cells was less synchronized to different extents (e.g. Fish 1 vs Fish 2). **(F)** Summary of the mean max cross-correlation coefficient values of calcium traces in each cell population of repeated *in vivo* calcium imaging assays ($n_{(\text{calcium sessions})}=16$, see Supplementary Fig. 1b for all measurements). The values for LH cells are significantly higher and more uniform than those of FSH cells (unpaired *t*-test, *** $p<0.0001$).

1.3. GnRH primarily activates LH cells

Next, we sought to characterize the response of the cells to GnRH, their putative common secretagogue. To determine the effect of GnRH on gonadotroph activity, we utilized an *ex vivo* preparation that preserves the brain-pituitary connection intact (Fig. 3A). Without stimulation, LH cells were either silent or exhibited small and short calcium transients (2-8.8 sec half-width, amplitude 0.23 -0.66 ∆F/F; Fig. 3B; Movie. S3A; Fig. S2, 7/10 fish) which were synchronized between small groups of neighbouring cells (2-14 cells per fish with a max cross-correlation coefficient > 0.5; Fig. S4). Independent of the basal activity of LH cells, in 80% of the fish, FSH cells elicited short and intense calcium bursts that had no clear organization (5.8-12.13 sec half-width, amplitude 0.63 - 1.03 ∆F/F; Fig. 3B, Fig. S3; Movie. S3C).

For stimulation, we applied a GnRH3 analog used for spawning induction in fish (*34*). In response to GnRH puff application (300 µl of 30 µg/µl), LH cells exhibited a strong and slow calcium rise (average half width 48.6 sec and average amplitude of 1.99 ∆F/F; Fig. 3C, Fig. S3; Movie. S3A and B), which was synchronized between the cells, as observed by the increase in correlation values from 0.26 ± 0.02 to 0.66 ± 0.05 (Fig. 3D). In contrast, in FSH cells only 50% of the fish displayed an increase in cross-correlation values from the basal state (Fig. 3D; Fig. S5A). Overall, whereas GnRH elicited a response in 95% of LH cells, only 56% of FSH cells responded to the treatment in the same fish (Fig. 3E). Due to this inconsistent response of FSH cells to GnRH stimuli we speculated that CCK might regulate their activity.

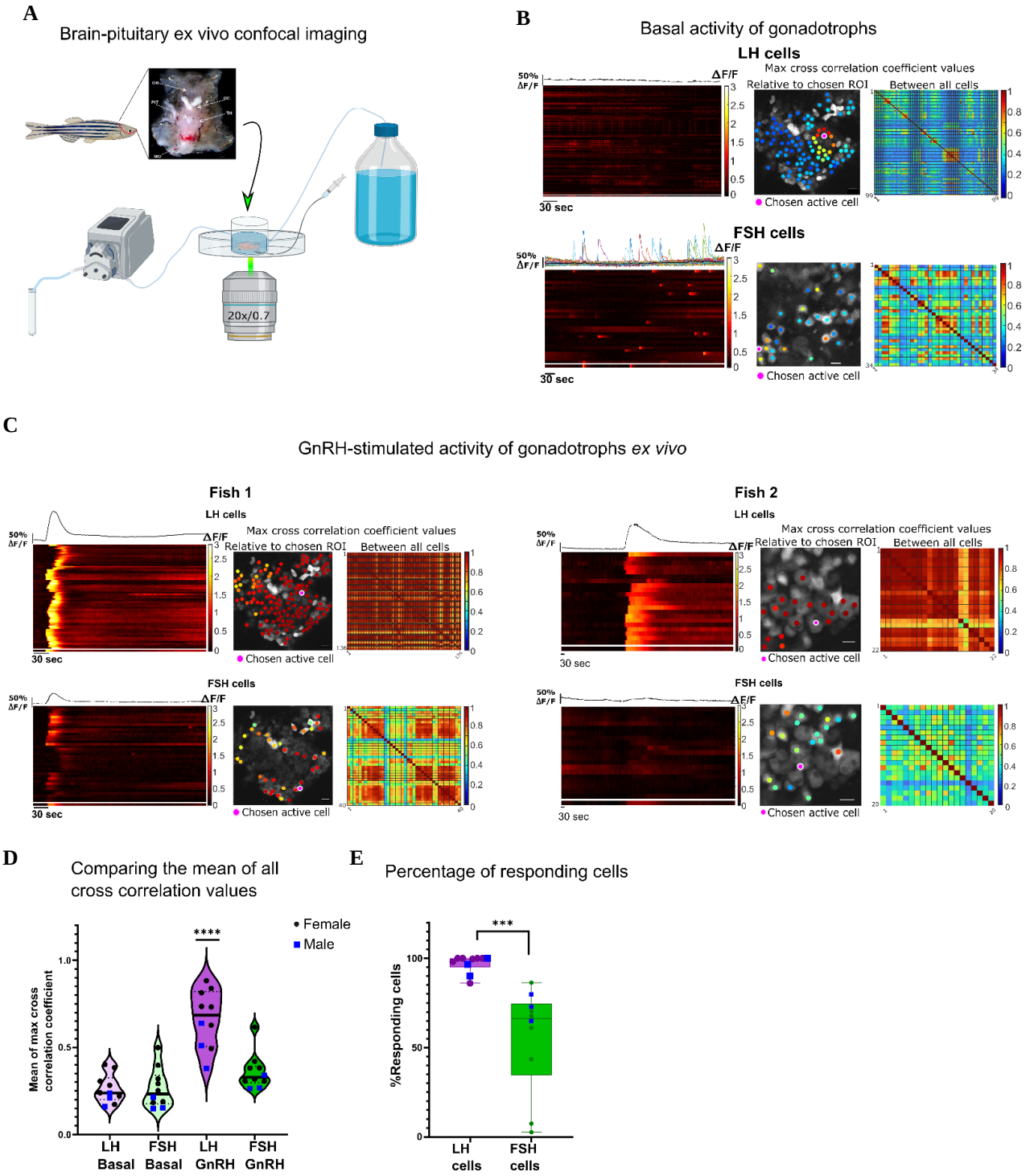

Fig. 3. GnRH induces a synchronized increase of calcium in all LH cells. (A) Top: Image of a dissected head with pituitary exposed from the ventral side of the fish used for the *ex vivo* assays (OB, olfactory bulb; OC, optic chiasm; PIT, pituitary; TH, thalamus; MO, medulla oblongata). Bottom: A diagram describing the *ex vivo* setup with a constant flow of artificial cerebrospinal fluid (ACSF), a side tube to inject stimuli, and a collecting tube. **(B)** A representative analysis of basal calcium activity of LH and FSH cells. The left panel is a heatmap of calcium traces (ΔF/F), where each line represents a cell, with the mean calcium trace on top, the separated line at the bottom of each heatmap is the calcium trace of the chosen ROI. The color-coded data points on the right are superimposed on the imaged cells and represent the maximum cross-correlation coefficient between a calcium trace of an active chosen ROI to those of the rest of the cells in the same population, matrix on the right represent the maximum cross-correlation coefficient values between all the cells. LH cells exhibited short calcium rises that were correlated between small groups of neighbouring cells (see supplementary fig. 3), whereas short, unorganized calcium

transients were observed in FSH cells (see supplementary fig. 2 for additional cell activity parameters). **(C)** An analysis of calcium response to GnRH stimulation in two representative imaging sessions. In all LH cells, a significant calcium rise was highly correlated. In 5/10 fish, a similar response to the stimulus was seen in FSH cells (see supplementary fig. 4 for detailed coefficient values distribution in each fish), albeit with lower calcium intensities and coefficient values (e.g., Fish 1), whereas in the other 5 fish FSH cells did not respond at all (e.g., Fish 2). **(D)** The mean of Max cross-correlation coefficient values in each cell type under each treatment (see supplementary fig. 4 for detailed coefficient values distribution in each fish) reveal that only LH cells are significantly affected by GnRH stimuli (n=10, 3 males, 7 females, one-way ANOVA, **** p<0.0001). **(E)** The percentage of cells responsive to GnRH stimulus (i.e., coefficient values higher than the 80 percentiles of basal values) is significantly higher in LH cells compared to FSH cells. Each dot represents one fish (n=10, 3 males, 7 females, unpaired *t*-test, *** p<0.001).

1.4. Cholecystokinin directly activates FSH cells

To functionally test the effect of CCK on gonadotroph activity, we applied the peptide (250 µl of 30 µg/ml CCK) to our ex vivo preparation and monitored the calcium response of the cells. CCK elicited a strong calcium response (40.3 to 172 sec half-width, mean amplitude of 1.44 ΔF/F) in FSH cells, while in some of the fish, a lower response was observed in LH cells (Fig. 4A and B; Fig. S5; Movie S4). In all analysed fish (n=7), all FSH cells responded to CCK, whereas the number of LH cells that responded to the stimulation varied widely (20%-100%, n=7; Fig. 4C). The calcium response in FSH cells was highly synchronized (mean max cross-correlation coefficient, 0.7±0.04; Fig. 4B; Fig. S5). By contrast, the response of LH cells to CCK application was characterized by low mean of max cross-correlation coefficient values (0.43±0.05; Fig. 4B; Fig. S5). These results indicate that in fish, CCK preferentially activates calcium rise in FSH cells, albeit with a weaker activation of LH cells.

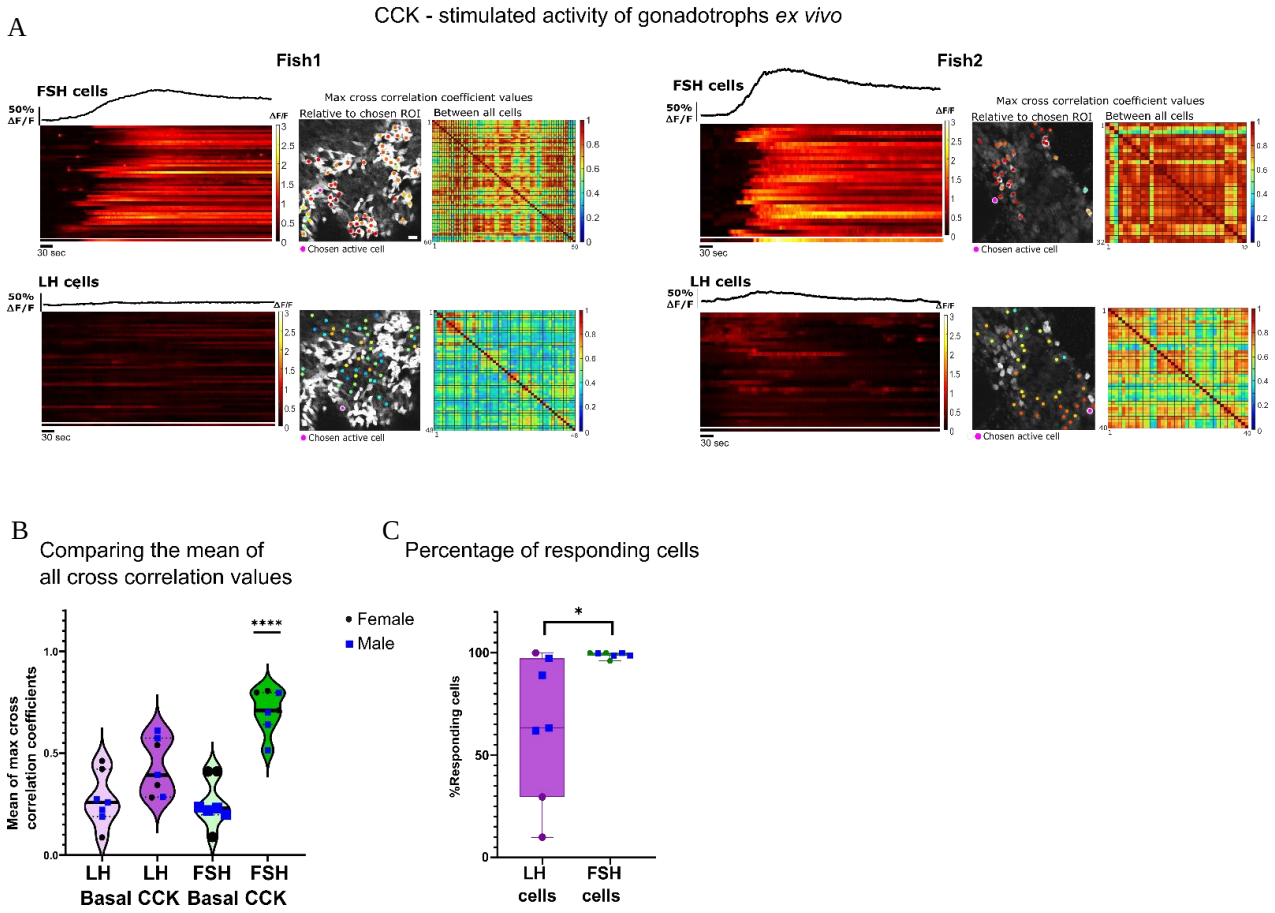

Fig. 4. FSH cells are directly stimulated by CCK. (A) Example of calcium analysis of FSH and LH cells during CCK stimulation: fish1 with only FSH cells responding, and fish2 with FSH and LH cells responding. For each fish the left panels are a heatmaps of calcium traces (ΔF/F), where each line represents a cell. On top of each heatmap is a graph showing the mean calcium trace, the separated line at the bottom of the heat map is the calcium trace of the chosen ROI. On the right are color-coded data points that are superimposed on the imaged cells, showing the maximum cross-correlation coefficient between a calcium trace of a chosen active ROI and those of the rest of the cells in the same population, next to it is a matrix of max cross correlation coefficients between all the cells. A high calcium rise (2.5 ∆F/F) was observed in FSH cells, while LH cells in some zebrafish responded with a very low amplitude. **(B)** The mean of max cross-correlation coefficient values in each cell type reveals that only FSH cells are significantly affected by CCK stimulation (n=7, 4 males, 3 females, one-way ANOVA, **** $p<0.0001$, see supplementary fig. 4 for detailed coefficient values distribution in each fish). **(C)** The percentage of active cells (i.e., a coefficient value higher than the 80 percentiles of basal levels) during CCK stimulation is significantly higher in FSH cells compared to LH cells. While in all the fish, 96%-100% of the FSH cells responded to CCK, in only half of the fish LH cells responded. Each dot represents one fish (n=7, 4 males, 3 females, unpaired *t*-test, * $p<0.05$).

1.5. Differential calcium response underlies differential hormone secretion

The calcium response observed in LH and FSH cells upon GnRH and CCK stimulation indicates a preferential stimulatory effect of the neuropeptides on each cell type., The effect of these neuropeptides on LH and FSH secretion was examined in order to determine the functional outcome of the stimulation. For that, we collected the medium perfused through our *ex vivo* system (Fig. 3A) and measured LH and FSH secretion levels using a specific ELISA validated for zebrafish GTHs (*35*) in parallel to monitoring the calcium activity of the cells. As expected, the calcium response to GnRH in LH cells was followed by a significant rise in LH secretion (Fig. 5A). In contrast, FSH cells responded with a very low calcium rise in hormonal secretion in response to GnRH treatment that was not significant from the basal secretion. Conversely, the application of CCK elicited a significant calcium rise in FSH cells followed by an elevation of FSH concentration in the medium, whereas in LH cells, no significant effect was observed on calcium, and the slight increase in LH secretion was not significant (n=5; Fig. 5B). These results were reproduced *in vivo*, as CCK injection significantly increased the expression and secretion of FSH (Fig. 5C and D) whereas the response to GnRH did not reach statistical significance ($p=0.069$). GnRH only affected LH expression in the pituitary (Fig. S6).

Taken together, these results suggest that GnRH and CCK preferentially activate calcium-dependent secretion in LH and FSH cells, respectively, and induce the release of these gonadotropins from the pituitary gland.

A

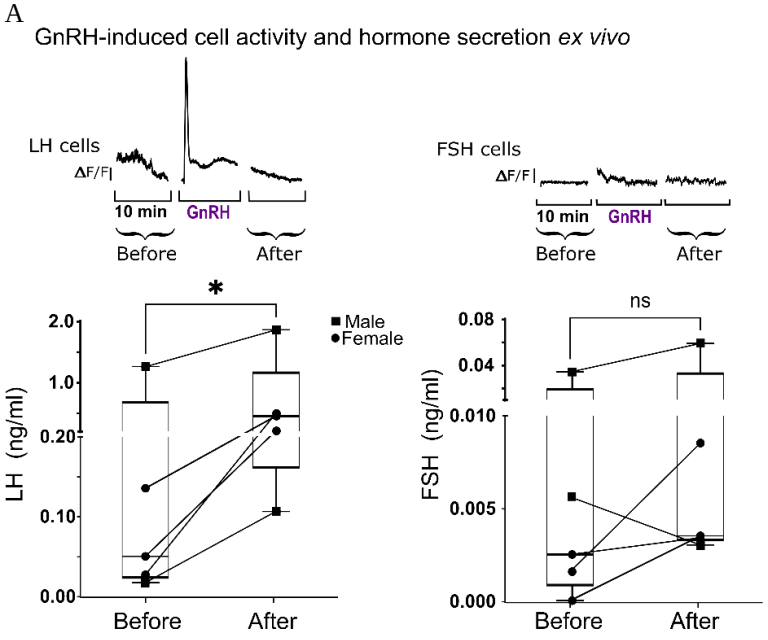
GnRH-induced cell activity and hormone secretion ex vivo
LH cells
ΔF/F
10 min
GnRH
Before
After
FSH cells
ΔF/F
10 min
GnRH
Before
After
*
Male
Female
LH (ng/ml)
2.0
1.0
0.20
0.10
0.00
Before
After
ns
FSH (ng/ml)
0.08
0.04
0.010
0.005
0.000
Before
After

B

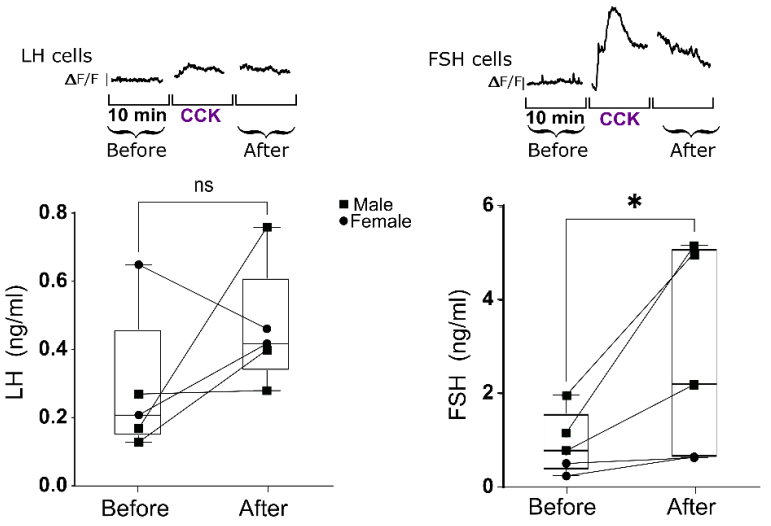
CCK-induced cell activity and hormone secretion ex vivo
LH cells
ΔF/F
10 min
CCK
Before
After
FSH cells
ΔF/F
10 min
CCK
Before
After
ns
Male
Female
LH (ng/ml)
0.8
0.6
0.4
0.2
0.0
Before
After
*
FSH (ng/ml)
6
4
2
0
Before
After

C

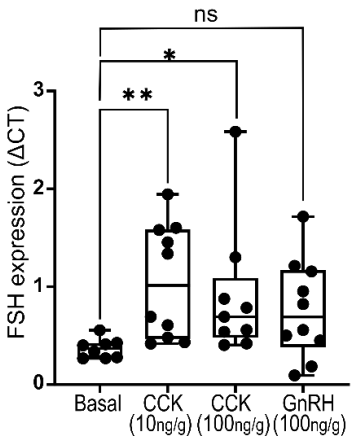
Transcription response to CCK and GnRH in vivo
ns
*
**
FSH expression (ΔCT)
3
2
1
0
Basal
CCK (10ng/g)
CCK (100ng/g)
GnRH (100ng/g)

D

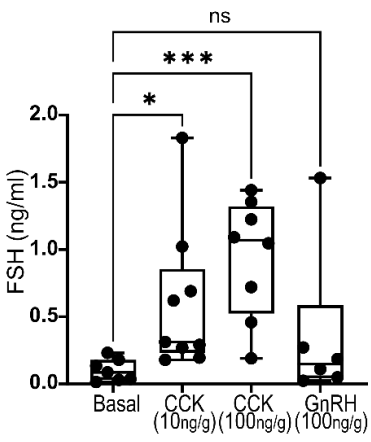
FSH secretion in response to CCK and GnRH in vivo
ns
***
*
FSH (ng/ml)
2.0
1.5
1.0
0.5
0.0
Basal
CCK (10ng/g)
CCK (100ng/g)
GnRH (100ng/g)

Fig. 5. The stimulated calcium activity of LH and FSH cells is associated with hormone secretion. **(A and B)** Top: Graphs showing mean calcium trace of 10 LH cells (left panel) or FSH cells (right panel) from consecutive imaging sessions before, during, and after the application of the stimulus (GnRH or CCK). Bottom: Secretion of LH or FSH before or after GnRH **(A)** or CCK **(B)** stimulation. Compared to basal levels, GnRH increased LH secretion, whereas CCK increased FSH secretion (dots from the same imaged pituitaries are connected with a line; n=5, paired t-test , *p<0.05). **(C)** Two hours after injection into live fish (n=10, 5 females and 5 males), CCK, but not GnRH, significantly increased the transcription of FSH in the pituitary (see Supplementary Fig. 4 for LH transcription; one-way ANOVA, * p<0.05, ** p<0.01). **(D)** FSH plasma levels increased significantly in a dose dependent manner after CCK injection (n=10, 5 females and 5 males), whereas GnRH injection did not affect FSH secretion (one-way ANOVA, * p<0.05, *** p<0.001).

Discussion

GnRH has long been considered the common stimulator of gonadotropin secretion in vertebrates. However, accumulating evidence for GnRH-independent FSH secretion in several mammalian species has questioned this regulatory role of GnRH (*36-39*). Moreover, in fish, normal ovarian development in hypophysiotropic GnRH loss-of-function mutants (*2, 27*), together with the lack of FSH cells response to GnRH stimuli in pituitary cell culture (*12*) further highlights the existence of an unknown FSH regulator other than GnRH. Here, we reveal that in zebrafish, CCK, a satiety hormone, gates reproduction by directly regulating GtH secretion. We show that GnRH preferentially controls LH secretion and identify CCK as the long-sought hypothalamic FSH secretagogue. Our results indicate that while fish gonadotrophs were segregated into two different populations and placed under the control of two distinct neuropeptides during evolution, a common hypothalamic pathway gates the secretion of both gonadotropins. Interestingly, in contrast to GnRH, the novel CCK regulation identified under the current study has a more substantial effect on the gonadotrophic axis, as revealed in our mutants, while the disruption of GnRH and its receptors didn't lead to any drastic effect on reproduction (*24, 40*).

The role of CCK as a satiety hormone has been demonstrated in multiple species of mammals and fish (*41-43*). From an evolutionary perspective, allocating a satiety hormone for gating reproduction serves the unique demands of the life history of oviparous species. Egg-laying and placental animals display a marked difference in their reproductive energy allocation strategies. In oviparous species, the pre-ovulatory processes of gonadal development involving vitellogenin synthesis and deposition into the developing oocyte, also known as folliculogenesis, constitute the main nutritional challenge during the female reproductive cycle. By contrast, in placental mammals, post-ovulatory pregnancy and milk production require the recruitment of the maternal metabolic pathways to accommodate the nutritional needs of the offspring. Thus, in oviparous species, folliculogenesis is gated by the animal's nutritional status, whereas in mammals, poor nutrition mainly restricts ovulation (*44, 45*). Since folliculogenesis and spermatogenesis are controlled by gonadotropin signaling from the pituitary, nutritional gating of gonadotrophs, may serve as an effective pathway to inhibit gonad development under limiting energetic balance. Our data suggest that, indeed, dedicated hypothalamic neurons have developed to integrate metabolic cues, such as food abundance and somatic condition, to induce the energetically costly process of reproduction in fish. Since CCK is a regulator of satiety in fish (*28, 42, 46*), this hypothalamic circuit directly links the metabolic status of the fish to its reproductive capacity (Fig. 6). Considering the recent report of an FSH-regulating role for CCK in the distantly related species medaka

(*47*), our findings represent a highly conserved mechanism for controlling reproduction in fish.

In the CCKR LOF mutants, gonad development was disrupted and led to an all-male population with underdeveloped testes. Female gonad development in fish is directly linked to FSH signalling activity, as shown by genetic mutation of FSH receptors that leads to female gonad arrest and differentiation into male gonads as the fish mature (*3*). The lack of females in our LOF mutant, together with the male's infertility, suggests a direct disruption of both LH and FSH circuitry. We further show that CCK directly controls FSH cells by innervating the pituitary gland and binding to specific receptors that are particularly abundant in FSH gonadotrophs. However, our calcium imaging results and the LOF mutants demonstrate that CCK also activates LH cells to some extent. This activation may either be direct, as LH cells were also shown to express the CCK receptor (*1*) albeit at a lower level, or indirect, by affecting LH cells via activation of GnRH or other neurons. The latter pathway can be wired through the close apposition of GnRH3 and CCK terminals in the zebrafish pituitary and was reported to exist in mammals (*48, 49*).

Our identification of CCK-producing axons innervating the zebrafish pituitary suggests a predominantly central CCK-dependent control of FSH release. Similar innervation was observed in ancient jawless fish, such as lamprey (*29*) and modern teleosts, such as the goldfish (*50*). Modern oviparous tetrapods were also shown to express the CCK receptor in their pituitary glands (*51*), indicating that this regulatory circuit may be evolutionarily conserved and common to oviparous vertebrates. However, since CCK is produced in the gut as well as in the central nervous system, we cannot rule out circulating CCK as a possible activator of GtH cells. Nevertheless, the direct innervation of CCK terminals into the pituitary gland and the concomitant increase of CCK in the gut and in the brain in response to feeding (*42, 52, 53*) suggest that the two sources of CCK are interconnected. In this context, the vagal nerve may serve as a possible gut-brain communication route, as it was shown to relay satiety signals to the hypothalamus via CCK (*54, 55*), thus forming a parasympathetic regulatory loop onto the hypothalamo-pituitary-gonadal axis.

Unlike the situation in fish, CCK LOF mice can reproduce (*43*), reflecting that the main metabolic challenge in the reproductive cycle of mammals is controlled by placental gonadotropins rather than by the hypothalamic-pituitary axis. The identified functional overlap in the hypothalamic control of both gonadotropins in fish efficiently serves to gate reproduction by a single neuropeptide. Importantly, similar functional overlap also exists in the potency of GnRH to activate FSH cells, corresponding to a previous finding where LH and FSH are co-secreted during the female spawning cycle (*56*). However, since FSH cells express a different type of GnRH receptor (*1*), their activation is less consistent and results in reduced gonadotropin secretion. Moreover, in the zebrafish, as well as in other species, the functional overlap in gonadotropin signaling pathways is not limited to the pituitary but is also present in the gonad, through the promiscuity of the two gonadotropin receptors (*56, 57*). This multilevel overlap creates functional redundancy that grants the reproductive system a high level of robustness and ensure the species' persistence .

Overall, our findings propose an updated view of the regulation of gonadal function in fish, in which metabolically driven hypothalamic circuits evolved to control gonad development. In addition to the novel insight into the evolution and function of the reproductive axis in oviparous animals, these findings are also of particular importance in

the context of aquaculture, which has become the dominant supplier of fish for human consumption in the face of declining yields from wild fisheries (*58, 59*). With the identification of the CCK circuit as a regulator of folliculogenesis and the main gateway between metabolic state and reproduction, novel tools targeting this pathway can now be designed to manipulate gonadal development and overcome challenges in gamete production and the control of puberty onset in farmed fish (*60, 61*).

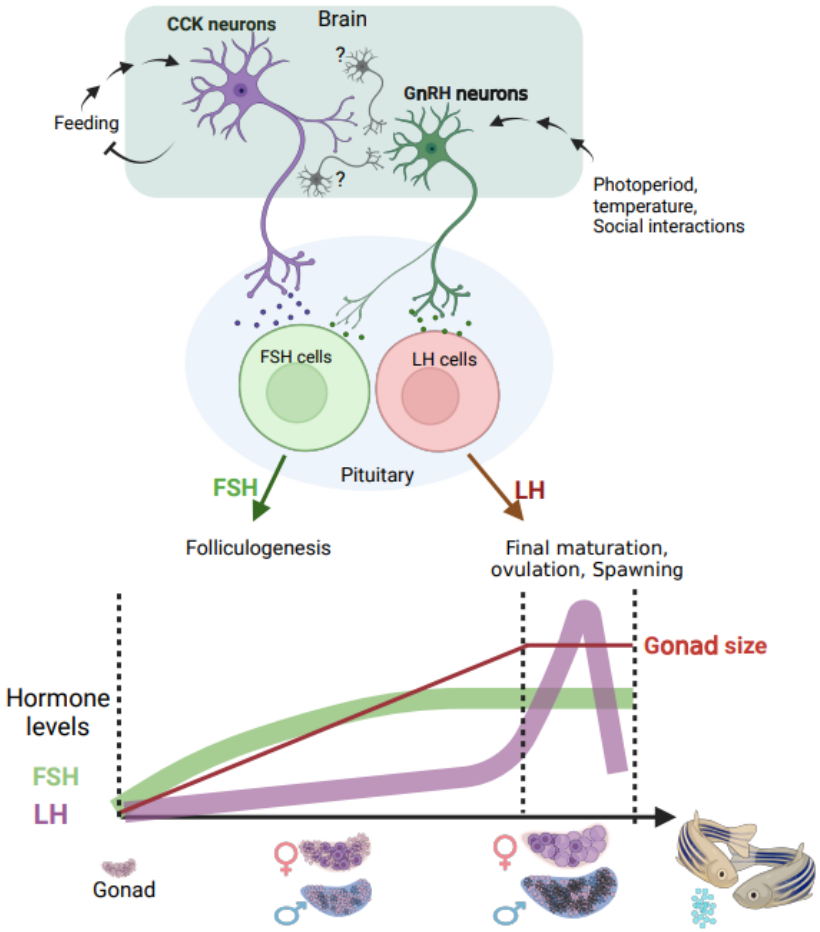

Fig. 6. A model summarizing the two suggested regulatory axes controlling fish reproduction. The satiety-regulated CCK neurons activate FSH cells . LH cells are directly regulated by GnRH neurons that are gated by CCK, photoperiod, temperature, and behaviour, eventually leading to final maturation and ovulation. Bottom image schematically represents the relative timescale of the two processes and the associated gonadotropin levels. (Created with BioRender.com)

Materials and Methods

1.1. Experimental design

To identify if CCK signaling affects the reproductive axis we compared a complete lose-of-function fish to their wt or heterozygous siblings that were grown under the exact same conditions. To identify the regulatory mechanism that allows the differential secretory activity of LH and FSH cells, we took advantage of the fact that in fish, these gonadotropic hormones are produced by two separate cell populations. Using the well-established model organism, the zebrafish, we simultaneously monitored the activity of

LH and FSH cells in a triple transgenic fish that expresses RCaMP2 under the regulation of both LH and FSH promoters, together with GFP under the regulation of FSH promoter. Because gonadotrophs control reproductive physiology, we used sexually mature fish that were at least six months old, contained mature gonads and exhibited reproductive behaviour. In each assay, the sex of each fish was determined by dissecting the gonads and identifying the morphology of eggs or sperm. We first characterized the *in vivo* calcium activity of the cells in an intact physiological environment. Then, we stimulated the pituitary with either GnRH or CCK and measured calcium activity. For that, we used isolated brains containing the pituitary, since no difference was observed in calcium activity of isolated pituitary or isolated brain and pituitary. Experimental units were either individual fish or GtH cells, depending on the experiment.

1.2. Sample size and replication

Sample size varied between experiments, depending on the number of transgenic fish allocated for each experiment. The minimum sample size was three.

1.3. Data inclusion/exclusion criteria

Fish were excluded from analysis if they showed no calcium activity or if tissue movements during the full recording session prevented reliable calcium analysis. Data or samples were not excluded from analysis for other reasons.

1.4. Randomization

Fish used for the experiments were randomly selected and randomly assigned to experimental groups. All GtH cells that could be detected in the selected fish were used for the analysis and thus, there was no requirement for randomization of cell selection.

1.5. Blinding

During experimentation and data acquisition, blinding was not applied to ensure tractability. Calcium data were quantified using a computational pipeline applied equally to all samples.

1.6. Animals

All experiments were approved by the Animal Welfare and Ethical Review Body of Languedoc-Roussillon (APAFIS#745-2015060114396791) and by the Experimentation Ethics Committee of the Hebrew University of Jerusalem (research number: AG-17-15126, Date: April 30, 2017). Zebrafish were housed according to standard conditions. Fertilized eggs were incubated at 28.5°C in E3 medium. For the current study, the transgenic line *tg(LH:RCaMP2,FSH:RCaMP2)* was generated by co-injection of two constructs (*FSH:RCaMP* and *LH:RCaMP*) to embryos, the positive F1 fish expressing RCaMP2 in both cell types were crossed again with *tg*(FSH:GFP) to generate the triple transgenic fish *tg(FSH:RCaMP2, FSH:GFP, LH:RCaMP2)* . Other transgenic lines used were *tg(FSH:GFP)* and *tg(GnRH:GFP)* and *tg(LH:RFP, FSH:GFP)* (*62*).

1.7. Plasmid construction

All expression plasmids were generated using the Tol2kit (*63*) and Gateway system (Invitrogen). Briefly, entry clones were generated by the addition of appropriate adaptors to DNA fragments via polymerase chain reaction (PCR) amplification. Amplicons were then recombined into donor vectors using BP recombination. A 5′-entry clone (p5E), a middle entry clone (pME), and a 3′-entry clone (p3E) were then recombined through an LR reaction into an expression vector carrying tol2-recognition sequences and either an

mCherry or a GFP heart marker (pDestTol2CG). The LH and FSH promoters (*62*) were cloned from Nile tilapia genomic DNA and inserted into pDONRP4-P1R to generate p5′-LH and p5’-FSH; those clones had been previously shown to be effective in marking LH and FSH cells in zebrafish (*30*). R-CaMP2 (*64*) was a gift from H. Bito (University of Tokyo) and was cloned into pDONR221 to generate pME-R-CaMP2. For GFP expression, the middle clone pME-EGFP was used. The expression vectors containing p5E-**LH**:PME-R-CaMP2:p3E-PolyA (red heart marker) and p5E-**FSH**:PME-R-CaMP2:p3E-PolyA (green heart marker) were co-injected to create *tg(LH&FSH:CaMP2)* fish, which were later crossed with *tg(FSH:GFP)* fish to generate the triple transgenic fish.

1.8. In vivo calcium imaging

Adult fish were anesthetized using 0.6 µM tricaine and immobilized by IP injection of 10 µl α-tubocurarine (5 mM; Sigma-Aldrich). To expose the pituitary, the jaw of the fish containing the dentary and part of the articular bones, together with a small slice from the mucosa overlying the palate, were removed by blunt dissection under a stereomicroscope, the total duration of the dissection was 10 to 15 minutes. The fish was then placed in a modified chamber, where the hyoid bone was gently pushed backward using a thin silver wire. A tube with a constant flow of fresh system water was placed in the jaw cavity in front of the gills. Heartbeat was monitored during calcium imaging as an indicator of viability. Each imaging session lasted 10 minutes and was repeated several times for each fish.
Calcium imaging was performed using a FVMPE RS two-photon microscope (Olympus) setup with an InSight X3 femtosecond-pulsed infrared laser (Spectra-Physics) and a 25×, numerical aperture 1.05 water-immersion objective (XLPLN25XWMP2, Olympus). The laser wavelength was tuned to 940 nm for GFP or 1040 nm for R-CaMP2. Calcium signals were recorded by time-lapse acquisition using galvanometric scanning mode and conventional raster scanning with a frequency up to 10 Hz.

1.9. Ex vivo calcium imaging

Adult fish were euthanized using ice-cold water and decapitated. The head was transferred to ice-cold ACSF (124 mM NaCl, 3 mM KCl, 2 mM $CaCl_2$, 2 mM $MgSO_4$, 1.25 mM NaH_2PO_4, 26 mM $NaHCO_3$, and 10 mM glucose (pH 7.2)) perfused with 5% CO_2 and 95% O_2. The heads were further dissected under a stereomicroscope. The ventral side of the head, including the jaw, gills and mucus, was removed using fine forceps and microscissors, the optic nerves were cut and the eyes were removed. Next, the bone at the base of the skull that covers the pituitary (sella turcica) was removed using fine forceps. The head was placed in a dedicated chamber (Fig. 3B) and stabilized with a slice anchor. The chamber had one inlet and one outlet, allowing for a constant flow of ACSF at a rate of 1 ml/minute, and an additional inlet that was placed in proximity to the tissue for injections of stimuli. The total volume of ACSF in the chamber was 3 ml. Imaging was performed in an inverted confocal fluorescent microscope (Leica SP8). R-CaMP2 activity was imaged at 4-10 Hz using the resonant scanner. The laser wavelength was 540 nm and the emission band was 630 nm. Images were taken using the ×20 objective. Each imaging session lasted 10 minutes. Before and after each session, the tissue was imaged once for GFP (excitation, 488 nm and emission, 530 nm) and R-CaMP2 (540 nm and 590 nm) in two separate channels. Images were processed using the Fiji program (*65*) for resolution using the Gaussian Blur filter and motion correction using the moco plugin (*66*).

To measure hormone secretion in response to salmon GnRH analogue [(D-Ala6,Pro9-Net)-mammalian GnRH (Bachem Inc., Torrance, CA) or fish CCK [(D-Y[SO3H]-L-G-W-M-D-F-NH2), synthesized by GL Biochem] stimulation, the medium was collected through the chamber outlet during the entire imaging session (10 ml per session in total). Each pituitary was imaged three times for 10 minutes: before, during and after stimulation. The stimulus was applied manually as a pulse of 300 µl of 30 µg/µl peptide during the first 30 seconds of the imaging session. Hormones were measured in the fractions before and after stimulation using ELISA developed for common carp, which was established in the Levavi-Sivan lab using recombinant carp gonadotropins produced in yeast, and had been previously shown to be suitable for zebrafish (24).
Tissue viability was validated by monitoring the morphology and activity of the cells, looking at granulation and calcium changes. This specific preparation was also viable two hours after dissection, when all the cells responded to the different stimuli.

1.10. Analysis of Ca2+ imaging data

A composite of GFP-positive and RCaMP-positive cells was created to distinguish between LH and FSH cells. Regions of interest corresponding to each cell in the imaged plane were manually drawn using Fiji. Two separated ROI sets were created, FSH cells (GFP-positive) and LH cells (R-CaMP2-positive and GFP-negative). Using the Fiji ROI manager, two datasets were created: a data sheet containing the mean grey values in each frame during the complete image sequence, and a data sheet containing the ROI centroids. Sheets and images were then processed using MATLAB R2017a.
Traces were normalized using the equation $\Delta F = \frac{Ft}{F0} - 1$, where $F0$ is the lowest value in the means calculated from every N frame in the complete trace (N= sampling frequency*5). When the sampling rate was higher than 4 Hz, we applied a low pass filter with a cut-off frequency of 2/ (sampling frequency /2).

1.11. Analysis of correlations coefficients between cells

Cross-correlation coefficients represent the maximum coefficient value between all cells or relative to a chosen ROI. From each set of traces, we obtained cross-correlation sequence ranges from -maxlag to maxlag and the values were normalized such that autocorrelations at 0 lag equalled 1. For each set we demonstrate only the maximum correlation values. The values are represented in a dot plot superimposed on the cells according to their centroid values when compared to the chosen ROI (pink dot), or as a heatmap when correlation is between all the cells. For violin plots, the mean of the maximum cross-correlation coefficient values in each fish were further visualized and analysed for statistical significance using Prism 9 (GraphPad, San Diego, CA).

1.12. HCR for CCKR and immunostaining of CCK

Staining was performed on whole head slices, as previously described (*67*). Briefly, whole heads were fixed overnight in 4% paraformaldehyde (PFA) and then decalcified for 4–7 days in 0.5 M EDTA at 4°C. Subsequently, heads were cryoprotected in 30% (wt/vol) sucrose, frozen in an OCT embedding compound and cryosectioned at a thickness of 15 µm. For immunostaining, head sections from transgenic zebrafish *tg(GnRH:GFP)* and *tg(FSH:GFP)* (*67*) were blocked with 5% normal goat serum for 1 h to reduce non-specific reactions. They were then incubated with rabbit anti-cholecystokinin (26-33) (CCK-8) antibody (diluted 1:1000, Merck, C2581) for 16 h at 4°C. The same antibody had been previously used to mark CCK-positive cells in the gut of the red drum fish (*68*). Antibodies were diluted in PBS with 1% BSA and 0.3% Triton X-100. The slides were rinsed three times with PBS for 5 min and were incubated for 2 h at

room temperature with goat anti-rabbit antibodies conjugated to Alexa674 fluorophore. HCR staining was performed according to the HCR RNA-FISH protocol for fresh-frozen or fixed-frozen tissue sections (*69*) (Molecular Instrument) on double-labelled transgenic fish *tg(LH:RFP, FSH:GFP)*. The detection stage was performed with probes against CCKR-like RNA (XM_017357750.2) and the amplification stage was performed using the 647 nm amplifier fluorophores. Sections were then counterstained with DAPI nuclear staining. After washing, slides were mounted with anti-fade solution (2% propyl gallate, 75% glycerol, in PBS) and imaged by confocal microscopy.

1.13. In vivo assay for CCK and GnRH injections

Six-month-old zebrafish (5 males and 5 females) were injected intraperitoneally with the following: 1) fish CCK peptide [(D-Y[SO3H]-L-G-W-M-D-F-NH2), synthesized by GL Biochem] at a concentration of 10 ng/g or 100 ng/g body weight, 2) salmon GnRH analogue [(D-Ala6,Pro9-Net)-mammalian GnRH (Bachem Inc., Torrance, CA) at a concentration of 100 ng/g body weight, 3) similar volumes of saline. Two hours post-injection, the fish were sedated using MS-222, bled from the heart as previously described (*70*), and decapitated. Pituitaries were dissected under a stereomicroscope and placed in Total RNA Isolation Reagent (Trizol). From each fish, between 15 µl and 20 µl of blood was collected. The blood was centrifuged at 970 × g 30 min and the plasma was separated and stored at −20°C. LH and FSH expression in the pituitary was measured using real-time PCR. RNA extraction, reverse transcription of RNA and real-time PCR were carried out as previously described (*13*). FSH secretion was measured in the plasma using ELISA for common carp, which was established in the Levavi Sivan lab using recombinant carp gonadotropins from in the yeast , and had been previously shown to be suitable for zebrafish (*35*).

1.14. Generating the LOF mutants of the cck receptor

CCKR LOF were generated using CRISPR-Cas9 technology. Three single guide RNAs (sgRNA, supplementary table 2) were designed using CHOPCHOP web tool (*71*) to specifically target coding regions in the CCKR gene (NCBI: XM_017357750.2; Fig. S1). Synthetic sgRNA (Sigma-Aldrich Israel Ltd) were co injected with Cas9 into single-cell stage zebrafish embryos. Mature injected zebrafish were screened for gene mutation using high-resolution melt (HRM) curve analysis (*72*) and bred with WT zebrafish to generate F1 heterozygous zebrafish. Out of the three designed sgRNA , guide number 2 was identified as the most efficient, creating the highest amount of mutated zebrafish. Mutated F1 heterozygous zebrafish were bred again to create the F2 generation containing a mix of genotypes: WT, heterozygous and homozygous zebrafish.
Mixed genotype F2 siblings from the same spawning event were reared in the same tanks until sexual maturity was identified (5-6 months). Tissues for H&E staining, RNA purification and genotyping were collected from three groups of siblings (n=47).
For the genotyping of the mutation, fin clips were collected, and DNA was extracted using HOTSHOT method (*73*), amplified by PCR and sequenced (sanger sequencing, Hylabs). Three types of mutations were identified and characterised for LOF: insertion of 12 nucleotides ($CCKR^{+12}$), insertion of 7 nucleotides ($CCKR^{+7}$) and depletion of one nucleotide ($CCKR^{-1}$; Fig. S6). LOF fish had contained one of the mutation types in each allele.
Pituitaries were collected for RNA purification and measured for LH and FSH expression using real-time PCR. RNA extraction, reverse transcription of RNA and real-time PCR were carried out as previously described (*13*).

The abdomen of the zebrafish was fixed in 4% PFA and sent for H&E staining (Gavish Research Services (GRS)). 4µm Slices of the abdomen containing the gonads were analysed using FIJI (*65*). The gonad area and the different cell types in the gonad were identified according to the 'Histology atlas of the zebrafish' (van der ven, wester P 2003)

1.15. Statistical analysis

Statistical analysis was performed using Prism 9 software (GraphPad). Whiskers on bar plots represent mean ± SEM**.** In violin plots, middle line represents the median, whereas the bottom and top lines represent the lower and upper quartiles, respectively**.** The datasets in all figures were tested for equal variances (using Bartlett's test) and normality (using D'Agostino and Pearson's test or Shapiro-Wilk test for smaller datasets). Dataset pairs that exhibited equal variances and normal distribution were compared using a two-tailed unpaired *t*-test (for two sets). For datasets with more than two sets we used one-way analysis of variance (ANOVA), followed by the Tukey-Kramer test. Datasets with different variances and/or non-Gaussian distributions were tested using two-tailed Mann-Whitney's test (for two sets) or Brown-Forsythe's one-way ANOVA, followed by Dunnett's T3 multiple comparisons test. To compare levels of secreted hormone in the *ex vivo* assay, the one-tailed paired *t*-test (Wilcoxon test) was performed, as the sample size was lower than 10. To compare the datasets of the *in vivo* assay of CCK and GnRH injections, and the gonadotrophs expression in the LOF fish, a nonparametric one-way ANOVA test (Kruskal-Wallis test) was used, as the datasets failed the Bartlett's test of equal variance. Significance was imparted at $P < 0.05$.

References

1. L. Hollander-Cohen, M. Golan, B. Levavi-Sivan, Differential Regulation of Gonadotropins as Revealed by Transcriptomes of Distinct LH and FSH Cells of Fish Pituitary. *Int J Mol Sci* **22**, (2021).
2. A. Takahashi, S. Kanda, T. Abe, Y. Oka, Evolution of the Hypothalamic-Pituitary-Gonadal Axis Regulation in Vertebrates Revealed by Knockout Medaka. *Endocrinology* **157**, 3994-4002 (2016).
3. Z. Zhang, S.-W. Lau, L. Zhang, W. Ge, Disruption of Zebrafish Follicle-Stimulating Hormone Receptor (fshr) But Not Luteinizing Hormone Receptor (lhcgr) Gene by TALEN Leads to Failed Follicle Activation in Females Followed by Sexual Reversal to Males. *Endocrinology* **156**, 3747-3762 (2015).
4. L. Chu, J. Li, Y. Liu, W. Hu, C. H. K. Cheng, Targeted gene disruption in zebrafish reveals noncanonical functions of LH signaling in reproduction. *Molecular Endocrinology* **28**, 1785-1795 (2014).
5. P. E. Belchetz, T. M. Plant, Y. Nakai, E. J. Keogh, E. Knobil, Hypophysial Responses to Continuous and Intermittent Delivery of Hypothalamic Gonadotropin-Releasing Hormone. *Science* **202**, 631-633 (1978).
6. R. Savoy-Moore, K. Swartz, "Several GnRH stimulation frequencies differentially release FSH and LH from isolated, perfused rat anterior pituitary cells" in *Regulation of Ovarian and Testicular Function* (Springer, 1987), pp. 641-645.
7. G. A. Stamatiades, U. B. Kaiser, Gonadotropin regulation by pulsatile GnRH: Signaling and gene expression. *Molecular and Cellular Endocrinology* **463**, 131-141 (2018).
8. I. R. Thompson, U. B. Kaiser, GnRH pulse frequency-dependent differential regulation of LH and FSH gene expression. *Molecular and cellular endocrinology* **385**, 28-35 (2014).
9. C. W. Yuen, W. Ge, Follistatin suppresses FSHbeta but increases LHbeta expression in the goldfish - evidence for an activin-mediated autocrine/paracrine system in fish pituitary. *Gen Comp Endocrinol* **135**, 108-115 (2004).

10. S. Aroua, G. Maugars, S. R. Jeng, C. F. Chang, F. A. Weltzien, K. Rousseau, S. Dufour, Pituitary gonadotropins FSH and LH are oppositely regulated by the activin/follistatin system in a basal teleost, the eel. *Gen Comp Endocrinol* **175**, 82-91 (2012).
11. Z. Yaron, G. Gur, P. Melamed, H. Rosenfeld, B. Levavi-Sivan, A. Elizur, Regulation of gonadotropin subunit genes in tilapia. *Comp Biochem Physiol B Biochem Mol Biol* **129**, 489-502 (2001).
12. S. W. Lin, W. Ge, Differential regulation of gonadotropins (FSH and LH) and growth hormone (GH) by neuroendocrine, endocrine, and paracrine factors in the zebrafish--an in vitro approach. *Gen Comp Endocrinol* **160**, 183-193 (2009).
13. J. Biran, S. Ben-Dor, B. Levavi-Sivan, Molecular identification and functional characterization of the kisspeptin/kisspeptin receptor system in lower vertebrates. *Biol Reprod* **79**, 776-786 (2008).
14. S.-W. Lin, W. Ge, Differential regulation of gonadotropins (FSH and LH) and growth hormone (GH) by neuroendocrine, endocrine, and paracrine factors in the zebrafish—an in vitro approach. *Gen Comp Endocrinol* **160**, 183-193 (2009).
15. K. Tsutsui, T. Ubuka, G. E. Bentley, L. J. Kriegsfeld, Gonadotropin-inhibitory hormone (GnIH): discovery, progress and prospect. *Gen Comp Endocrinol* **177**, 305-314 (2012).
16. J. Biran, M. Golan, N. Mizrahi, S. Ogawa, I. S. Parhar, B. Levavi-Sivan, LPXRFa, the Piscine Ortholog of GnIH, and LPXRF Receptor Positively Regulate Gonadotropin Secretion in Tilapia (Oreochromis niloticus). *Endocrinology* **155**, 4391-4401 (2014).
17. J. Biran, M. Golan, N. Mizrahi, S. Ogawa, I. S. Parhar, B. Levavi-Sivan, Direct regulation of gonadotropin release by neurokinin B in tilapia (Oreochromis niloticus). *Endocrinology* **155**, 4831-4842 (2014).
18. S. Ogawa, M. Sivalingam, J. Biran, M. Golan, R. S. Anthonysamy, B. Levavi-Sivan, I. S. Parhar, Distribution of LPXRFa, a gonadotropin-inhibitory hormone ortholog peptide, and LPXRFa receptor in the brain and pituitary of the tilapia. *The Journal of comparative neurology* **524**, 2753-2775 (2016).
19. Y. Cohen, K. Hausken, Y. Bonfil, M. Gutnick, B. Levavi-Sivan, Spexin and a Novel Cichlid-Specific Spexin Paralog Both Inhibit FSH and LH Through a Specific Galanin Receptor (Galr2b) in Tilapia. *Frontiers in endocrinology* **11**, 71 (2020).
20. K. Mitchell, W. S. Zhang, C. Lu, B. Tao, L. Chen, W. Hu, V. L. Trudeau, Targeted mutation of secretogranin-2 disrupts sexual behavior and reproduction in zebrafish. *Proceedings of the National Academy of Sciences* **117**, 12772-12783 (2020).
21. J. J. Rajeswari, S. Unniappan, Phoenixin-20 Stimulates mRNAs Encoding Hypothalamo-Pituitary-Gonadal Hormones, is Pro-Vitellogenic, and Promotes Oocyte Maturation in Zebrafish. *Sci Rep* **10**, 6264 (2020).
22. J. A. Tello, S. Wu, J. E. Rivier, N. M. Sherwood, Four functional GnRH receptors in zebrafish: analysis of structure, signaling, synteny and phylogeny. *Integrative and Comparative Biology* **48**, 570-587 (2008).
23. K. Okubo, Y. Nagahama, Structural and functional evolution of gonadotropin-releasing hormone in vertebrates. *Acta Physiol (Oxf)* **193**, 3-15 (2008).
24. S. Tanaka, N. Zmora, B. Levavi-Sivan, Y. Zohar, Chemogenetic Depletion of Hypophysiotropic GnRH Neurons Does Not Affect Fertility in Mature Female Zebrafish. *Int J Mol Sci* **23**, (2022).
25. O. S. Spicer, T.-T. Wong, N. Zmora, Y. Zohar, Targeted Mutagenesis of the Hypophysiotropic Gnrh3 in Zebrafish (Danio rerio) Reveals No Effects on Reproductive Performance. *PLOS ONE* **11**, e0158141 (2016).
26. K. E. Whitlock, J. Postlethwait, J. Ewer, Neuroendocrinology of reproduction: Is gonadotropin-releasing hormone (GnRH) dispensable? *Frontiers in Neuroendocrinology* **53**, 100738 (2019).
27. M. Marvel, O. S. Spicer, T. T. Wong, N. Zmora, Y. Zohar, Knockout of the Gnrh genes in zebrafish: effects on reproduction and potential compensation by reproductive and feeding-related neuropeptides. *Biol Reprod* **99**, 565-577 (2018).
28. B. A. Himick, R. E. Peter, CCK/gastrin-like immunoreactivity in brain and gut, and CCK suppression of feeding in goldfish. *Am J Physiol* **267**, R841-851 (1994).
29. D. Sobrido-Cameán, L. A. Yáñez-Guerra, D. Robledo, E. López-Varela, M. C. Rodicio, M. R. Elphick, R. Anadón, A. Barreiro-Iglesias, Cholecystokinin in the central nervous system of the

sea lamprey Petromyzon marinus: precursor identification and neuroanatomical relationships with other neuronal signalling systems. *Brain Struct Funct* **225**, 249-284 (2020).
30. M. Golan, A. O. Martin, P. Mollard, B. Levavi-Sivan, Anatomical and functional gonadotrope networks in the teleost pituitary. *Scientific Reports* **6**, 23777 (2016).
31. Z. Zhang, B. Zhu, W. Ge, Genetic Analysis of Zebrafish Gonadotropin (FSH and LH) Functions by TALEN-Mediated Gene Disruption. *Molecular Endocrinology* **29**, 76-98 (2015).
32. L. Chu, J. Li, Y. Liu, C. H. K. Cheng, Gonadotropin Signaling in Zebrafish Ovary and Testis Development: Insights From Gene Knockout Study. *Molecular Endocrinology* **29**, 1743-1758 (2015).
33. M. Inoue, A. Takeuchi, S. Horigane, M. Ohkura, K. Gengyo-Ando, H. Fujii, S. Kamijo, S. Takemoto-Kimura, M. Kano, J. Nakai, K. Kitamura, H. Bito, Rational design of a high-affinity, fast, red calcium indicator R-CaMP2. *Nat Methods* **12**, 64-70.
34. Y. Zohar, C. C. Mylonas, Endocrine manipulations of spawning in cultured fish: from hormones to genes. *Aquaculture* **197**, 99-136 (2001).
35. L. Hollander-Cohen, M. Golan, J. Aizen, M. Shpilman, B. Levavi-Sivan, Characterization of carp gonadotropins: Structure, annual profile, and carp and zebrafish pituitary topographic organization. *Gen Comp Endocrinol* **264**, 28-38 (2018).
36. S. M. McCann, S. Karanth, C. A. Mastronardi, W. L. Dees, G. Childs, B. Miller, S. Sower, W. H. Yu, Control of Gonadotropin Secretion by Follicle-Stimulating Hormone-Releasing Factor, Luteinizing Hormone-Releasing Hormone, and Leptin. *Archives of Medical Research* **32**, 476-485 (2001).
37. V. Padmanabhan, K. McFadden, D. T. Mauger, F. J. Karsch, A. R. Midgley, Jr., Neuroendocrine Control of Follicle-Stimulating Hormone (FSH) Secretion. I. Direct Evidence for Separate Episodic and Basal Components of FSH Secretion1. *Endocrinology* **138**, 424-432 (1997).
38. M. D. Culler, A. Negro-Vilar, Pulsatile follicle-stimulating hormone secretion is independent of luteinizing hormone-releasing hormone (LHRH): pulsatile replacement of LHRH bioactivity in LHRH-immunoneutralized rats. *Endocrinology* **120**, 2011-2021 (1987).
39. K. Y. Pau, P. M. Gliessman, T. Oyama, H. G. Spies, Disruption of GnRH pulses by anti-GnRH serum and phentolamine obliterates pulsatile LH but not FSH secretion in ovariectomized rabbits. *Neuroendocrinology* **53**, 382-391 (1991).
40. O. S. Spicer, T. T. Wong, N. Zmora, Y. Zohar, Targeted Mutagenesis of the Hypophysiotropic Gnrh3 in Zebrafish (Danio rerio) Reveals No Effects on Reproductive Performance. *PLoS One* **11**, e0158141 (2016).
41. M. Lõhmus, P. A. Raven, L. F. Sundström, R. H. Devlin, Disruption of seasonality in growth hormone-transgenic coho salmon (Oncorhynchus kisutch) and the role of cholecystokinin in seasonal feeding behavior. *Hormones and Behavior* **54**, 506-513 (2008).
42. X. Zhang, N. Tang, J. Qi, S. Wang, J. Hao, Y. Wu, H. Chen, Z. Tian, B. Wang, D. Chen, Z. Li, CCK reduces the food intake mainly through CCK1R in Siberian sturgeon (Acipenser baerii Brandt). *Sci Rep* **7**, 12413 (2017).
43. C. M. Lo, A. King, L. C. Samuelson, T. L. Kindel, T. Rider, R. J. Jandacek, H. E. Raybould, S. C. Woods, P. Tso, Cholecystokinin knockout mice are resistant to high-fat diet-induced obesity. *Gastroenterology* **138**, 1997-2005 (2010).
44. C. J. Ashworth, L. M. Toma, M. G. Hunter, Nutritional effects on oocyte and embryo development in mammals: implications for reproductive efficiency and environmental sustainability. *Philos Trans R Soc Lond B Biol Sci* **364**, 3351-3361 (2009).
45. S. D. Torre, V. Benedusi, R. Fontana, A. Maggi, Energy metabolism and fertility—a balance preserved for female health. *Nature Reviews Endocrinology* **10**, 13-23 (2014).
46. H. Volkoff, The role of neuropeptide Y, orexins, cocaine and amphetamine-related transcript, cholecystokinin, amylin and leptin in the regulation of feeding in fish. *Comparative Biochemistry and Physiology Part A: Molecular & Integrative Physiology* **144**, 325-331 (2006).
47. S. K. Uehara, Y. Nishiike, K. Maeda, T. Karigo, S. Kuraku, K. Okubo, S. Kanda, Cholecystokinin is the follicle-stimulating hormone (FSH)-releasing hormone. *bioRxiv*, 2023.2005.2026.542428 (2023).

48. P. Giacobini, A. S. Kopin, P. M. Beart, L. D. Mercer, A. Fasolo, S. Wray, Cholecystokinin Modulates Migration of Gonadotropin-Releasing Hormone-1 Neurons. *The Journal of Neuroscience* **24**, 4737-4748 (2004).
49. P. Giacobini, S. Wray, Cholecystokinin Directly Inhibits Neuronal Activity of Primary Gonadotropin-Releasing Hormone Cells through Cholecystokinin-1 Receptor. *Endocrinology* **148**, 63-71 (2007).
50. B. A. Himick, R. E. Peter, CCK/gastrin-like immunoreactivity in brain and gut, and CCK suppression of feeding in goldfish. *American Journal of Physiology-Regulatory, Integrative and Comparative Physiology* **267**, R841-R851 (1994).
51. Y. Wan, Q. Deng, Z. Zhou, Y. Deng, J. Zhang, J. Li, Y. Wang, Cholecystokinin (CCK) and its receptors (CCK1R and CCK2R) in chickens: functional analysis and tissue expression. *Poultry Science* **102**, 102273 (2023).
52. A. S. Gomes, E. Lygre, T. Harboe, F. Zimmermann, A.-E. O. Jordal, K. Hamre, I. Rønnestad, The role of cholecystokinin and peptide YY in feed intake in Atlantic halibut (Hippoglossus hippoglossus) larvae. *Neuropeptides* **91**, 102202 (2022).
53. G. D'Agostino, D. J. Lyons, C. Cristiano, L. K. Burke, J. C. Madara, J. N. Campbell, A. P. Garcia, B. B. Land, B. B. Lowell, R. J. Dileone, L. K. Heisler, Appetite controlled by a cholecystokinin nucleus of the solitary tract to hypothalamus neurocircuit. *eLife* **5**, e12225 (2016).
54. D. Borgmann, E. Ciglieri, N. Biglari, C. Brandt, A. L. Cremer, H. Backes, M. Tittgemeyer, F. T. Wunderlich, J. C. Brüning, H. Fenselau, Gut-brain communication by distinct sensory neurons differently controls feeding and glucose metabolism. *Cell Metabolism* **33**, 1466-1482.e1467 (2021).
55. C. Clemmensen, T. D. Müller, S. C. Woods, H.-R. Berthoud, R. J. Seeley, M. H. Tschöp, Gut-Brain Cross-Talk in Metabolic Control. *Cell* **168**, 758-774 (2017).
56. W.-K. So, H.-F. Kwok, W. Ge, Zebrafish Gonadotropins and Their Receptors: II. Cloning and Characterization of Zebrafish Follicle-Stimulating Hormone and Luteinizing Hormone Subunits—Their Spatial-Temporal Expression Patterns and Receptor Specificity1. *Biology of Reproduction* **72**, 1382-1396 (2005).
57. L. Hollander-Cohen, B. Böhm, K. Hausken, B. Levavi-Sivan, Ontogeny of the specificity of gonadotropin receptors and gene expression in carp. *Endocrine Connections* **8**, 1433-1446 (2019).
58. H. E. Froehlich, C. A. Runge, R. R. Gentry, S. D. Gaines, B. S. Halpern, Comparative terrestrial feed and land use of an aquaculture-dominant world. *Proceedings of the National Academy of Sciences* **115**, 5295-5300 (2018).
59. J. L. Anderson, F. Asche, T. Garlock, J. Chu, "Aquaculture: Its role in the future of food" in *World agricultural resources and food security* (Emerald Publishing Limited, 2017).
60. Y. Zohar, Endocrinology and fish farming: Aspects in reproduction, growth, and smoltification. *Fish Physiology and Biochemistry* **7**, 395-405 (1989).
61. G. L. Taranger, M. Carrillo, R. W. Schulz, P. Fontaine, S. Zanuy, A. Felip, F.-A. Weltzien, S. Dufour, Ø. Karlsen, B. Norberg, E. Andersson, T. Hansen, Control of puberty in farmed fish. *Gen Comp Endocrinol* **165**, 483-515 (2010).
62. M. Golan, J. Biran, B. Levavi-Sivan, A novel model for development, organization and function of gonadotropes in fish pituitary. *Frontiers in endocrinology* **5**, 182 (2014).
63. K. M. Kwan, E. Fujimoto, C. Grabher, B. D. Mangum, M. E. Hardy, D. S. Campbell, J. M. Parant, H. J. Yost, J. P. Kanki, C.-B. Chien, The Tol2kit: A multisite gateway-based construction kit for Tol2 transposon transgenesis constructs. *Developmental Dynamics* **236**, 3088-3099 (2007).
64. H. Dana, B. Mohar, Y. Sun, S. Narayan, A. Gordus, J. P. Hasseman, G. Tsegaye, G. T. Holt, A. Hu, D. Walpita, R. Patel, J. J. Macklin, C. I. Bargmann, M. B. Ahrens, E. R. Schreiter, V. Jayaraman, L. L. Looger, K. Svoboda, D. S. Kim, Sensitive red protein calcium indicators for imaging neural activity. *eLife* **5**, e12727 (2016).
65. J. Schindelin, I. Arganda-Carreras, E. Frise, V. Kaynig, M. Longair, T. Pietzsch, S. Preibisch, C. Rueden, S. Saalfeld, B. Schmid, J. Y. Tinevez, D. J. White, V. Hartenstein, K. Eliceiri, P. Tomancak, A. Cardona, Fiji: an open-source platform for biological-image analysis. *Nat Methods* **9**, 676-682 (2012).

66. A. Dubbs, J. Guevara, R. Yuste, moco: Fast Motion Correction for Calcium Imaging. *Front Neuroinform* **10**, 6-6 (2016).
67. M. Golan, E. Zelinger, Y. Zohar, B. Levavi-Sivan, Architecture of GnRH-Gonadotrope-Vasculature Reveals a Dual Mode of Gonadotropin Regulation in Fish. *Endocrinology* **156**, 4163-4173 (2015).
68. K. A. Webb, Jr., I. A. Khan, B. S. Nunez, I. Rønnestad, G. J. Holt, Cholecystokinin: molecular cloning and immunohistochemical localization in the gastrointestinal tract of larval red drum, Sciaenops ocellatus (L.). *Gen Comp Endocrinol* **166**, 152-159 (2010).
69. H. M. T. Choi, M. Schwarzkopf, M. E. Fornace, A. Acharya, G. Artavanis, J. Stegmaier, A. Cunha, N. A. Pierce, Third-generation in situ hybridization chain reaction: multiplexed, quantitative, sensitive, versatile, robust. *Development* **145**, (2018).
70. J. Biran, O. Palevitch, S. Ben-Dor, B. Levavi Sivan, Neurokinin B and neurokinin B receptor: a novel system involved in controlling fish reproduction. *PNAS* **109**, 10269-10274 (2012).
71. K. Labun, T. G. Montague, M. Krause, Y. N. Torres Cleuren, H. Tjeldnes, E. Valen, CHOPCHOP v3: expanding the CRISPR web toolbox beyond genome editing. *Nucleic Acids Research* **47**, W171-W174 (2019).
72. A. Segev-Hadar, T. Slosman, A. Rozen, A. Sherman, A. Cnaani, J. Biran, Genome Editing Using the CRISPR-Cas9 System to Generate a Solid-Red Germline of Nile Tilapia (Oreochromis niloticus). *The CRISPR Journal* **4**, 583-594 (2021).
73. N. D. Meeker, S. A. Hutchinson, L. Ho, N. S. Trede, Method for isolation of PCR-ready genomic DNA from zebrafish tissues. *Biotechniques* **43**, 610-614 (2007).

Acknowledgments

The writers would like to acknowledge the contribution of Mr Antony Pinot from the Mollard lab for its help in operating the two-photon microscopy, Einat Zelinger and Daniel Waiger from the CSI Center for Scientific Imaging Faculty of Agriculture for, for their help in guidance in operating the confocal microscopy. The authors would like to thank Dr. Zohar Gavish at Gavish Research Services for performing the histological work.

Funding: IPAM-BCM Platform, member of the national infrastructure France-BioImaging supported by the French National Research Agency (ANR-10-INBS-04).
The Israel Science Foundation (ISF) support (grant number 1540/17).
The U.S.-Israel Binational Science Foundation (Joint Funding Research Grants # NSF-BSF-1947541).

Author contributions:

Conceptualization: LHC, MG, BLS, PM.
Methodology: LHC, MG, BLS, PM, OR.
Investigation: LHC, OC, MS, TA, PF.
Visualization: LHC.
Supervision: BLS, PM, MG.
Writing—original draft: LHC, MG.
Writing—review & editing: MG, BLS, PM.